The Effects of Probe-Induced Flow Distortion on Atmospheric Turbulence Measurements: Extension to Scalars

J. C. WYNGAARD

National Center for Atmospheric Research, Boulder, Colorado*

(Manuscript received 9 March 1988, in final form 23 May 1988)

ABSTRACT

I.prove that in a steady velocity field the frequency spectrum of a conservative scalar is unaffected by flow distortion. This is a good approximation in turbulent flow if $(qa^{1/3}/U_1 l^{1/3}) \ll 1$, where q and l are velocity and length scales of the energy-containing turbulence, a is the crosstream dimension of the body, and U_1 is the mean flow speed. Rapid-distortion theory gives the same result under more restrictive conditions. Both sets of criteria seem easily met for scalar mixing ratio measurements in typical aircraft applications but are more difficult to satisfy on towers.

At aircraft speeds, crosstalk from air density fluctuations can seriously contaminate species density signals measured in regions of strong flow distortion. These errors can be very important in aircraft measurements of the vertical fluxes of CO_2 and water vapor, whose sensors typically measure species density rather than mixing ratio. These errors can be minimized through boom design.

Temperature measurements from aircraft can also be seriously affected by flow distortion; an error in the fluctuating temperature signal is generated by the exchange of kinetic energy and enthalpy during the flow distortion process. Appearing in the temperature signal as crosstalk from velocity fluctuations, the error is proportional to the amount of flow distortion and the deviation of the sensor recovery factor from 1.0.

1. Introduction

An earlier paper (Wyngaard 1981) presented a simple theory for the effects of probe-induced flow distortion on turbulent velocity statistics. Here, "probe-induced" means upstream of the sensor body, where the streamlines are distorted but there are no complicating effects of the trailing turbulent wake, as illustrated in Fig. 1. The theory is applicable when the turbulence integral scale is much larger than the scale of the distorting body, the usual case with in situ measurement of energy-containing-range statistics in the atmospheric surface layer. Hogstrom (1982) has since used the theory to interpret the performance of turbulence sensors. Wyngaard et al. (1985) extended it to axisymmetric bodies (e.g., aircraft), and Wyngaard (1988) used it to derive design criteria for turbulent flux sensors.

This paper further extends the theory to the measurement of turbulent scalars such as temperature and the concentration of trace species. Some scalar sensors, such as most Lyman-α devices for water vapor, tend to restrict the air flow through the measurement path. Such flow deformation clearly changes the *spatial* structure of the advected scalar field, as illustrated in Fig. 2.

Turbulence measurements from research aircraft have traditionally been made from forward-pointing nose booms. However, booms often have undesirable vibration characteristics, usually are too short to eliminate flow distortion effects completely, and can disturb the signals from nose-mounted radars. For these and other reasons the "nose radome" technique for measuring air motion is attractive. The probe in this case consists of an array of pressure ports in a nose radome; the conversion to velocity is made as in a conventional differential-pressure flow sensor. Early tests of the technique (Brown et al. 1983) have been quite encouraging. In converting from a nose boom system to the nose radome, however, one is forced to consider relocating sensors for scalars such as temperature, water vapor, and trace constituents to regions of strong flow distortion.

Although flow distortion changes the spatial statistics of scalars, researchers do not usually measure spatial statistics; instead, they infer them from measurements at a single point through Taylor's hypothesis (Lumley 1965), which assumes that a time series at a fixed point in a turbulent flow results from the advection of a "frozen" spatial pattern past that point by the mean velocity. Both this velocity and the spatial structure it advects are changed by the flow distortion. This raises

* The National Center for Atmospheric Research is sponsored by the National Science Foundation.

Corresponding author address: Dr. John C. Wyngaard, NCAR/MMM, P.O. Box 3000, Boulder, CO 80307-3000.

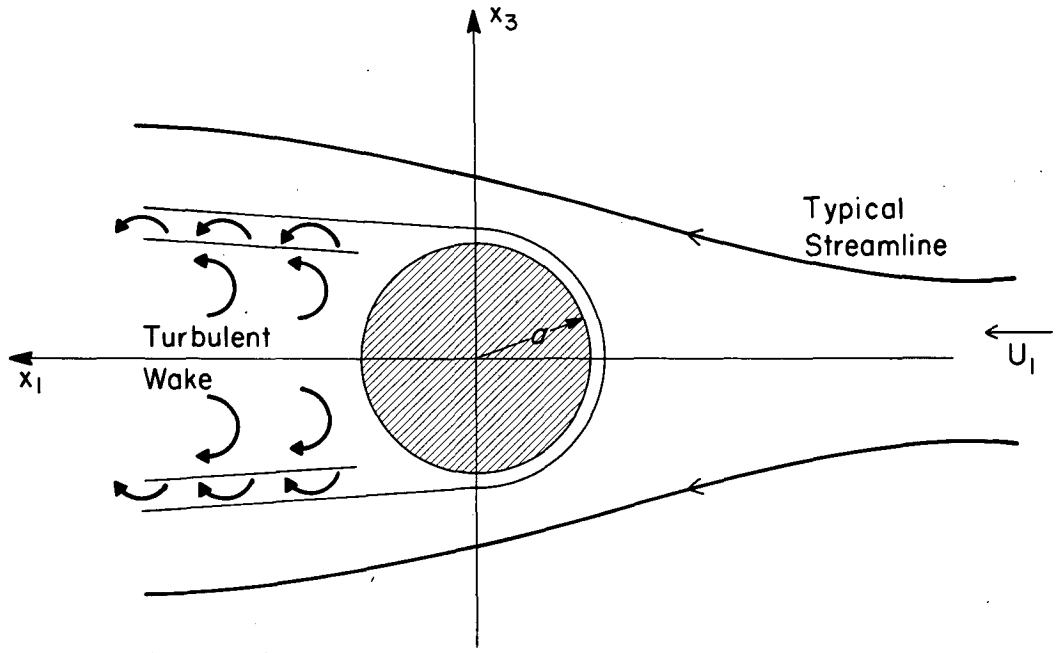

FIG. 1. A schematic of flow near a circular cylinder. The flow in the trailing wake is complicated and unpredictable in detail, but the flow ahead of the cylinder can be easily calculated if the integral scale l in the free stream is much larger than the cylinder radius a. From Wyngaard (1986).

the central question: What is the relation between the time series of a scalar in a region of flow distortion and that in the free stream?

2. The influence of flow distortion on the time series of a conservative scalar

a. The definition of a conservative scalar

We define a conservative scalar quantity C as one that satisfies the conservation equation

$$\frac{DC}{Dt} = \frac{\partial C}{\partial t} + U_j \frac{\partial C}{\partial x_j} = 0. \tag{1}$$

In general, the mass density ρ_s of a scalar constituent that has no sources or sinks satisfies the conservation equation

$$\frac{\partial \rho_s}{\partial t} + \frac{\partial \rho_s U_j}{\partial x_j} = \alpha \frac{\partial^2 \rho_s}{\partial x_j \partial x_j}, \tag{2}$$

where repeated indices are summed and α is the molecular diffusivity for ρ_s. In the large Reynolds and Peclet number flow in the lower atmosphere the molecular diffusion term in (2) is negligible for all but the smallest scales of motion, and at the low speeds typically met by tower-mounted sensors we can assume (Lumley and Panofsky 1964) that the divergence of the velocity vanishes (i.e., $\partial U_i/\partial x_i = 0$). Equation (2) then reduces to the form (1), so that these approximations imply that ρ_s is effectively conservative. Since ρ, the mass density of air, also satisfies (2), the assumption $\partial U_i/\partial x_i = 0$ also implies that air acts as an incompressible fluid.

Research aircraft velocities are typically an order of magnitude or more larger than wind speeds in the lower atmosphere, and the dynamically induced density changes at these higher speeds can be appreciable. Therefore incompressibility can be a questionable assumption for measurements from aircraft, and a scalar mass density might be considered conservative in in situ micrometeorological applications but not in aircraft applications. Even if ρ_s and ρ are not individually conservative, however, one can show from (2) and the negligibility of the molecular diffusion terms that the mixing ratio ρ_s/ρ is a conservative variable.

b. Theory for steady flow

Let C be a conservative scalar, such as water vapor mixing ratio, satisfying the conservation equation (1). We assume it is being measured by a probe whose bulk distorts the air flow, and for simplicity we model the problem as flow past a sphere (Fig. 3). We use spatial coordinates x_i, $i = 1, 2, 3$ fixed with respect to the body, as shown in Fig. 3. In the aircraft case, these coordinates are related to the usual Eulerian coordinates fixed with respect to the Earth by a Galilean transformation involving U_i, the constant velocity of the aircraft with respect to the Earth.

We denote the distorted scalar field by $\tilde{C}(x, t)$, and reserve $C(x, t)$ for the scalar field in the free stream. Similarly, we denote the distorted velocity field by $\tilde{U}_i$.

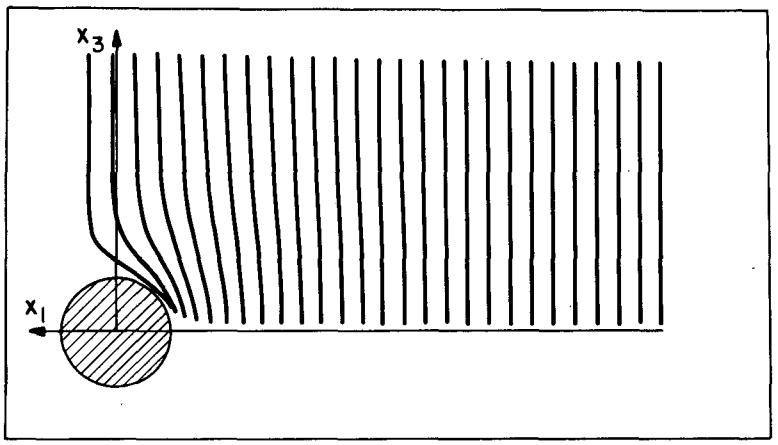

FIG. 2. The distortion of a conservative scalar field in steady flow around a circular cylinder. A streamwise periodic scalar distribution exists in the undistorted upstream flow, so that isoscalar lines are vertical there. As the flow decelerates along the x_1 axis the scalar contours are compressed, while near the top of the cylinder the acceleration spreads the contours. From Wyngaard (1986).

The conservation equation for the distorted scalar gradient $\partial\tilde{C}/\partial x_i = \tilde{C}_{,i}$ is derived by differentiating the $\tilde{C}$-equation with respect to x_i:

$$\frac{\partial \tilde{C}_{,i}}{\partial t} + \frac{\partial}{\partial x_i}\tilde{C}_{,j}\tilde{U}_j = 0. \tag{3}$$

This can be written as

$$\frac{D\tilde{C}_{,i}}{Dt} = -\frac{\partial \tilde{U}_j}{\partial x_i}\tilde{C}_{,j} \tag{4}$$

which confirms that the scalar gradient is not conserved during flow distortion.

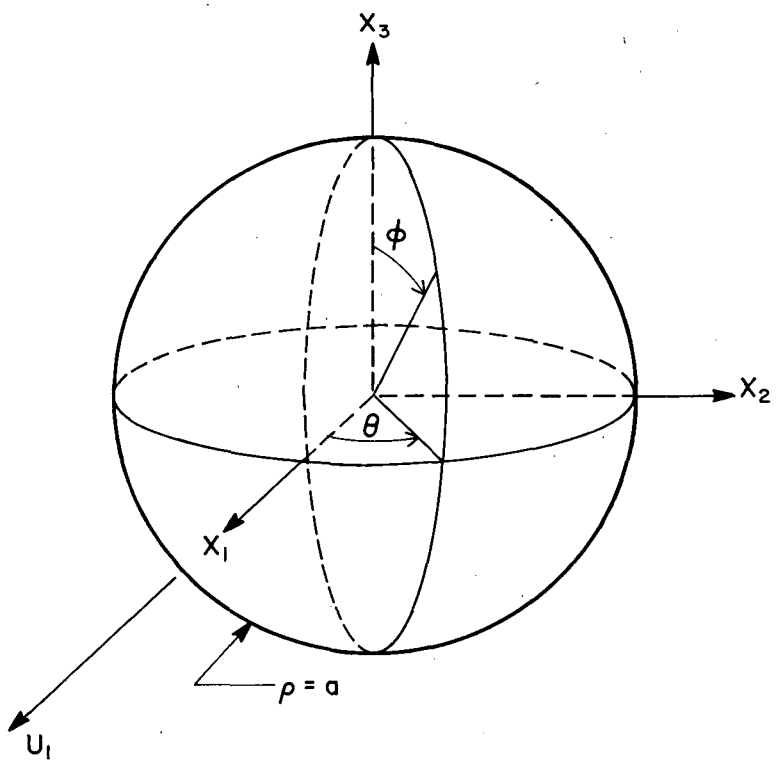

FIG. 3. The coordinate system for flow past a sphere.

If we multiply (3) by $\tilde{U}_i$ and change dummy indices, we find

$$\frac{\partial \tilde{C}_{,i}\tilde{U}_i}{\partial t} + \tilde{U}_j \frac{\partial \tilde{C}_{,i}\tilde{U}_i}{\partial x_j} = \frac{D\tilde{C}_{,i}\tilde{U}_i}{Dt} = \tilde{C}_{,i}\frac{\partial \tilde{U}_i}{\partial t}. \quad (5)$$

If the flow is steady, so that $\partial \tilde{U}_i/\partial t = 0$, (5) shows that the quantity $\tilde{C}_{,i}\tilde{U}_i$ is conserved during flow distortion; this means that any change in velocity due to flow distortion is accompanied by a compensating change in scalar gradient. Integrating (5) along a trajectory from $\mathbf{x}_0$ in the free stream to the measurement point $\mathbf{x}_m$ then gives

$$\tilde{C}_{,i}\tilde{U}_i(\mathbf{x}_m, t + \Delta t) = C_{,i}U_i(\mathbf{x}_0, t), \quad (6)$$

where Δt is the travel time. Using (1) in the free stream and in the distortion region gives

$$\frac{\partial C}{\partial t} + C_{,j}U_j = \frac{\partial \tilde{C}}{\partial t} + \tilde{C}_{,j}\tilde{U}_j = 0, \quad (7)$$

which with (6) gives

$$\frac{\partial C}{\partial t}(\mathbf{x}_0, t) = \frac{\partial \tilde{C}}{\partial t}(\mathbf{x}_m, t + \Delta t). \quad (8)$$

Thus, we conclude that in a steady velocity field, the time series of scalar fluctuations in the free stream and in the flow-distortion region are simply shifted in time by Δt. Therefore, the frequency spectra are identical.

c. *Theory for quasi-steady turbulent flow, low frequencies*

We now allow the free stream flow U_i to be the sum of a statistically stationary, turbulent component u_i (of order q, the square root of the turbulent kinetic energy) and a steady mean component U_1 in the x_1 direction. From (5), the equation for conservation of $C_{,i}U_i$ now becomes

$$\frac{DC_{,i}U_i}{Dt} = C_{,i}\frac{\partial u_i}{\partial t}. \quad (9)$$

If we integrate this over time following a trajectory that begins at $\mathbf{x}_0$ in the free stream and ends at the measurement point $\mathbf{x}_m$, we have

$$\tilde{C}_{,i}\tilde{U}_i(\mathbf{x}_m, t + \Delta t) - C_{,i}U_i(\mathbf{x}_0, t) = \left\langle C_{,i}\frac{\partial u_i}{\partial t}\right\rangle \Delta t, \quad (10)$$

where the angle brackets mean the average over the trajectory. Using (1) gives

$$\frac{\partial C}{\partial t}(\mathbf{x}_0, t) - \frac{\partial \tilde{C}}{\partial t}(\mathbf{x}_m, t + \Delta t) = \left\langle C_{,i}\frac{\partial u_i}{\partial t}\right\rangle \Delta t. \quad (11)$$

Because the flow is not steady the upstream point $\mathbf{x}_0$ is a random variable, fluctuating about a mean position because of the turbulent velocity u_i. We will discuss the implications of this later.

The terms in (11) are zero-mean, fluctuating signals of very wide bandwidth. We can estimate their peak frequencies by using Taylor's hypothesis to relate time and streamwise spatial (x_1) derivatives:

$$\frac{\partial u_i}{\partial t} \approx -U_1\frac{\partial u_i}{\partial x_1}; \quad \frac{\partial C}{\partial t} \approx -U_1\frac{\partial C}{\partial x_1}. \quad (12)$$

Since the variances of the spatial derivatives in (12) are proportional to the dissipation rates of turbulent energy and scalar variance (Tennekes and Lumley 1972), the spectra of $\partial C/\partial t$ and $\partial u_i/\partial t$ peak at about one-tenth the Kolmogorov frequency $f_k = U_1/(2\pi\eta)$ (Champagne et al. 1977). Here $\eta = (\nu^3/\epsilon)^{1/4}$ is the Kolmogorov microscale, where ν is the kinematic viscosity and ϵ is the dissipation rate of turbulent kinetic energy. In the atmospheric boundary layer, typically, $\eta \sim 1$ mm, and for values of U_1 between 5 and 100 m s^{-1} this means the spectral peaks of $\partial C/\partial t$ and $\partial u_i/\partial t$ lie between about 80 Hz and 1.6 kHz. Because most C-sensors do not have nearly this bandwidth, we will restrict our attention to lower frequencies by formally low-pass filtering Eq. (11). If we are interested in flux measurements and obtain the fluctuating velocity from a nose radome, we would expect degradation in the velocity signal beyond the probe frequency $f_p = U_1/(2\pi a)$. Similar considerations hold for most tower-based sensors. Thus, f_p is an appropriate cut-off frequency for our low-pass filter. In aircraft applications we might have $U_1 = 100$ m s^{-1}, $a = 1$ m, $f_p = 16$ Hz; in tower measurements $U_1 = 5$ m s^{-1}, $a = 0.2$ m, $f_p = 4$ Hz might be typical.

Filtering the left side of (11) is straightforward. The right side, however, is a nonlinear combination of random variables. As an estimate of the rms order of magnitude of its low-pass filtered form, we write

$$\left(\left\langle C_{,i}\frac{\partial u_i}{\partial t}\right\rangle \Delta t\right)^f \approx U_1\left(\left\langle C_{,i}\frac{\partial u_i}{\partial x_1}\right\rangle \Delta t\right)^f \approx \frac{\partial C^f}{\partial t} \times \frac{\partial u_i{}^f}{\partial x_1} \times \frac{a}{U_1}, \quad (13)$$

where a superscript f denotes a filtered signal. We now estimate the rms order of magnitude of the filtered $\partial u_i/\partial x_1$ signal as follows. The velocity derivative variance is of the order of the integral of $\kappa_1{}^2$ times the one-dimensional wavenumber spectrum $\phi_{\alpha\alpha}$ up to the Kolmogorov wavenumber, i.e.,

$$\overline{\left(\frac{\partial u_\alpha}{\partial x_1}\right)^2} \approx \int_0^{1/\eta} \kappa_1{}^2\phi_{\alpha\alpha}\,d\kappa_1 \approx \int_0^{1/\eta} \kappa_1{}^2\epsilon^{2/3}\kappa_1{}^{-5/3}\,d\kappa_1 \approx \epsilon^{2/3}\eta^{-4/3} \approx \frac{\epsilon}{\nu}, \quad (14)$$

where the overbar means ensemble average and κ_1 is the streamwise wavenumber. The filtered variance is therefore proportional to the integral up to the filter wavenumber:

$$\overline{\left(\frac{\partial u_\alpha^f}{\partial x_1}\right)^2} \approx \int_0^{1/a} \kappa_1^2 \phi_{\alpha\alpha} d\kappa_1 \approx \epsilon^{2/3} a^{-4/3} \approx (q^3/l)^{2/3} a^{-4/3}. \quad (15)$$

Here we have used $\epsilon \sim q^3/l$, where l is an energy-containing-range scale of u_i (Tennekes and Lumley 1972). Thus, we have from (13) and (15)

$$\left(\left\langle C_{,i} \frac{\partial u_i}{\partial t}\right\rangle \Delta t\right)^f \approx \frac{\partial C^f}{\partial t} \times O\left(\frac{q}{l^{1/3} a^{2/3}}\right) \times \frac{a}{U_1} \approx \frac{\partial C^f}{\partial t} \times O\left(\frac{q a^{1/3}}{U_1 l^{1/3}}\right). \quad (16)$$

Combining (11) and (16) then gives

$$\frac{\partial C^f}{\partial t} - \frac{\partial \tilde{C}^f}{\partial t} \approx \frac{\partial C^f}{\partial t} \times O\left(\frac{q a^{1/3}}{U_1 l^{1/3}}\right). \quad (17)$$

Thus, to measure scalar time series reliably at frequencies below f_p we need the parameter $(q a^{1/3})/(U_1 l^{1/3})$ to be small. In aircraft applications, typically $q \sim 1$ m s^{-1}, and $U_1 \sim 100$ m s^{-1}, so $q/U_1 \sim 10^{-2}$. The scale l usually lies between the distance from the surface and the depth of the PBL. If we take l as 300 m, and if $a = 1$ m, then this parameter is about 0.001, which should be small enough to neglect. In tower applications, q/U_1 is much larger, say 0.2. In a neutral surface layer l, as we have defined it, is about six times the distance from the surface; at a measurement height of 10 m, and with $a = 0.2$ m, $(q a^{1/3})/(U_1 l^{1/3}) = 0.03$. Each of these should be small enough to neglect, so that to a good approximation we expect

$$\frac{\partial \tilde{C}^f}{\partial t}(t + \Delta t) \approx \frac{\partial C^f}{\partial t}(t), \quad (18)$$

and we can take the frequency spectra at the measurement point $\mathbf{x}_m$ and at the point $\mathbf{x}_0$ in the free stream as identical below the probe frequency $f_p = U_1/(2\pi a)$.

We now deal with a point mentioned earlier: the turbulent component of the flow velocity makes $\mathbf{x}_0$, the free stream point of origin of the trajectories passing through the measurement point $\mathbf{x}_m$ at time Δt later, a random variable. In effect, this makes our problem one of measuring a turbulent scalar field in an undistorted free stream but with a probe having random displacements d_i from a location $\overline{\mathbf{x}_0}$. This probe motion multiplies the Fourier components of the scalar field by the factor $\exp(i\kappa_i d_i) \sim \exp(i\kappa_i u_i \Delta t)$ where κ_i is wavenumber. This introduces only phase shift into the scalar signal and, hence, does not change its spectrum. The cospectrum of the scalar and a signal that is not identically phase shifted (vertical velocity, say) will be distorted for $\kappa_i u_i \Delta t \geq 1$. Taylor's hypothesis then indicates that the frequency cospectrum will be distorted above the frequency $f_d = (U_1/q) f_p \gg f_p$. Thus, we conclude that at frequencies less than f_p the effect of this apparent probe motion is negligible.

d. *Theory for unsteady flow, high frequencies*

Under certain conditions the response of free-stream turbulence to the deformed streamlines around a body can be treated by what is called "rapid distortion" theory (Hunt 1973). This theory was originally developed by Batchelor and Proudman (1954) to calculate the changes produced in a homogeneous turbulent field subjected to a rapid, spatially uniform distortion, such as occurs when turbulent fluid flowing in a duct encounters an abrupt change in cross-sectional area. While Hunt (1973) has shown that in the case of turbulent flow approaching bluff bodies the spatial nonuniformity of the distortion greatly complicates the analysis, making the original, elegant solution of Batchelor and Proudman inapplicable in detail, it does hold qualitatively. Thus, we will extend the Batchelor–Proudman rapid-distortion analysis to a conservative scalar field.

As the turbulent scalar field approaches the probe, which we assume is axisymmetric, it encounters the mean strain field $\partial \tilde{U}_i/\partial x_j$. This distorts the scalar "eddies", as we saw in Fig. 2. Meanwhile, the scalar field is being continuously distorted by the strain rates of the turbulent velocity field in which it is imbedded, and smoothed by the molecular diffusion occurring on its wrinkled, contorted interfaces.

Following the classical work of Batchelor and Proudman (1954), we assume that distortion is so rapid that the turbulent strain rate q/λ acting on the scalar field is much smaller than the mean strain rate U_1/a. Here, $\lambda = (\nu q^2/\epsilon)^{1/2}$ is the Taylor microscale. The classical theory indicates that in order to neglect molecular diffusion effects during the distortion, the "eddy-turnover" time l/q, where l is the integral scale of the turbulent velocity field, must be much larger than the time of application of the mean strain, a/U_1. Thus, these criteria require, in order,

$$\frac{q}{\lambda} \ll \frac{U_1}{a}, \qquad \frac{l}{q} \gg \frac{a}{U_1}. \quad (19)$$

It may be surprising that the molecular diffusivity does not appear here, but it is well known (Tennekes and Lumley 1972) that dissipation rates in turbulence are set by the energy-containing range dynamics, and are independent of molecular diffusivity as long as it is nonzero.

Equations (19) are equivalent to

$$\frac{qa}{U_1\lambda} \ll 1,$$

$$\frac{qa}{U_1 l} \ll 1. \tag{20}$$

The Taylor microscale λ lies toward the small end of inertial subrange scales; within the planetary boundary layer (PBL) it is typically of the order of 0.1 m. Using that value and $q = 1$ m s^{-1}, $a = 1$ m, and $U_1 = 100$ m s^{-1} gives $qa/(U_1\lambda) = 0.1$ in typical aircraft applications. In the tower case with $q = 1$ m s^{-1}, $a = 0.2$ m, $U_1 = 5$ m s^{-1}, and $\lambda = 0.1$ m this parameter is 0.4. If we can interpret "$\ll$" as smaller by a factor of 10, the first equation of (20) is typically met in the aircraft case but not on the towers. The second criterion is much looser, since $l \gg \lambda$. Thus, our rapid distortion criteria would seem to be typically met for aircraft measurements within the PBL.

Let us then model the problem as axisymmetric, spatially uniform, rapid distortion of a turbulent scalar field. The approximation of spatially uniform distortion means that we must restrict ourselves to scalar eddy sizes not large compared to the body size a.

The conservation of C can be expressed as $\tilde{C}(\mathbf{x}, t) = C(\mathbf{a})$, where $\boldsymbol{x}$ is the location at time t of a fluid particle that was at position $\mathbf{a}$ at $t = 0$. This implies that C values before and after rapid distortion are related by

$$\frac{\partial \tilde{C}}{\partial x_i}\frac{\partial x_i}{\partial a_j} = \frac{\partial C}{\partial a_j}. \tag{21}$$

Here $\mathbf{a}$ and $\mathbf{x}$ are the positions of a given fluid particle before and after the distortion, respectively. We take both fields to be homogeneous and use the Fourier-Stieltjes representations

$$C(\mathbf{a}) = \int e^{i\boldsymbol{\kappa}\cdot\mathbf{a}} d\hat{C}(\boldsymbol{\kappa}),$$

$$\tilde{C}(\mathbf{x}) = \int e^{i\boldsymbol{\chi}\cdot x} d\hat{\tilde{C}}(\boldsymbol{\chi}), \tag{22}$$

where a hat denotes the Fourier-Stieltjes component and κ_i and χ_i are the wavenumber vectors in the undistorted and distorted fields, respectively. Substituting (22) into (21) and using $\boldsymbol{\chi}\cdot\mathbf{x} = \boldsymbol{\kappa}\cdot\mathbf{a}$ gives

$$i\chi_i \frac{\partial x_i}{\partial a_j} d\hat{\tilde{C}}(\boldsymbol{\chi}) = i\kappa_j d\hat{C}(\boldsymbol{\kappa}), \tag{23}$$

which by multiplying by $\partial a_j/\partial x_p$ can be written as

$$i\chi_p d\hat{\tilde{C}}(\boldsymbol{\chi}) = i\kappa_j \frac{\partial a_j}{\partial x_p} d\hat{C}(\boldsymbol{\kappa}). \tag{24}$$

Now since $\kappa_j a_j = \chi_m x_m$, we have

$$\kappa_j \frac{\partial a_j}{\partial x_p} = \chi_m \frac{\partial x_m}{\partial x_p} = \chi_p, \tag{25}$$

so that we can write (24) as

$$d\hat{\tilde{C}}(\boldsymbol{\chi}) = d\hat{C}(\boldsymbol{\kappa}), \tag{26}$$

which means that the distortion changes the wavenumbers of the Fourier components of the scalar field but not their amplitudes. The corresponding spectral relation is

$$\tilde{\phi}(\boldsymbol{\chi})d\boldsymbol{\chi} = \phi(\boldsymbol{\kappa})d\boldsymbol{\kappa}, \tag{27}$$

and if we integrate over all wavenumbers we see that the scalar variance is conserved during distortion:

$$\overline{\tilde{C}^2} = \overline{C^2}. \tag{28}$$

We now choose our coordinates to be the principal axes of the mean strain. We then have

$$\frac{\partial x_1}{\partial a_1} = e_1,\ \frac{\partial x_2}{\partial a_2} = e_2,\ \frac{\partial x_3}{\partial a_3} = e_3,\ \frac{\partial x_i}{\partial a_j} = 0 \text{ if } i \neq j$$

$$\frac{\partial a_1}{\partial x_1} = \frac{1}{e_1},\ \frac{\partial a_2}{\partial x_2} = \frac{1}{e_2},\ \frac{\partial a_3}{\partial x_3} = \frac{1}{e_3},\ \frac{\partial a_i}{\partial x_j} = 0 \text{ if } i \neq j \tag{29}$$

$$e_1 e_2 e_3 = 1$$

One can show that $d\boldsymbol{\chi} = d\boldsymbol{\kappa}$, so that $\phi(\boldsymbol{\kappa}) = \tilde{\phi}(\boldsymbol{\chi})$, and, consequently,

$$\int \tilde{\phi}(\boldsymbol{\chi})d\chi_2 d\chi_3 = \int \phi(\boldsymbol{\kappa})d\chi_2 d\chi_3$$

$$= \int \phi(\boldsymbol{\kappa}) \frac{\partial a_2}{\partial x_2}\frac{\partial a_3}{\partial x_3} d\kappa_2 d\kappa_3. \tag{30}$$

The one-dimensional, streamwise spectra of the undistorted and distorted scalar fields are therefore related by

$$\tilde{\phi}_1(\chi_1) = \frac{\partial a_2}{\partial x_2}\frac{\partial a_3}{\partial x_3}\phi_1(\kappa_1). \tag{31}$$

We model the process along the stagnation streamline ahead of the probe as an axisymmetric expansion, for which

$$\frac{\partial a_1}{\partial x_1} = \frac{1}{e_1} > 1,$$

$$\frac{\partial a_2}{\partial x_2} = \frac{\partial a_3}{\partial x_3} = e_1^{1/2} < 1. \tag{32}$$

Ahead of a two-dimensional body we would have a two-dimensional expansion, where

$$\left.\begin{aligned}\frac{\partial a_1}{\partial x_1} &= \frac{1}{e_1} > 1,\\ \frac{\partial a_2}{\partial x_2} &= e_1 < 1,\\ \frac{\partial a_3}{\partial x_3} &= 0\end{aligned}\right\}. \tag{33}$$

Thus, in each case we have

$$\tilde{\phi}_1(\chi_1) = \tilde{\phi}_1\left(\frac{\kappa_1}{e_1}\right) = e_1\phi_1(\kappa_1), \tag{34}$$

or, equivalently,

$$\tilde{\phi}_1(\kappa_1) = e_1\phi_1(\kappa_1 e_1). \tag{35}$$

The wavenumbers of interest here will in most cases be inertial, so we take the undistorted one-dimensional spectrum to be

$$\phi_1(\kappa_1) \sim \kappa_1^{-5/3}. \tag{36}$$

Equation (35) then shows that the distorted spectrum is

$$\tilde{\phi}_1(\kappa_1) = e_1^{-2/3}\phi_1(\kappa_1). \tag{37}$$

Since $e_1 < 1$, this indicates that a rapid expansion amplifies the streamwise wavenumber spectrum of a conservative scalar in the inertial subrange. A rapid contraction, which could be considered to occur in the off-axis, accelerating flow around the body, would attenuate the inertial range wavenumber spectrum.

Let us examine the implications of our results for frequency spectra. Taylor's hypothesis in the form $\kappa_1 = 2\pi f/U_1$, plus the constraint that both frequency and streamwise wavenumber spectra must integrate to the variance, imply that the two spectra are related by

$$S(f) = \frac{2\pi}{U_1}\phi_1\left(\frac{2\pi f}{U_1}\right). \tag{38}$$

Thus, from (35) and (38) we can write the distorted frequency spectrum as

$$\tilde{S}(f) = \frac{2\pi}{\tilde{U}_1}\tilde{\phi}_1\left(\frac{2\pi f}{\tilde{U}_1}\right) = \frac{2\pi}{\tilde{U}_1}e_1\phi_1\left(\frac{2\pi f e_1}{\tilde{U}_1}\right). \tag{39}$$

Since $e_1 = \tilde{U}_1/U_1$, we can rewrite (39) as

$$\tilde{S}(f) = \frac{2\pi}{U_1}\phi_1\left(\frac{2\pi f}{U_1}\right) = S(f). \tag{40}$$

Thus, even though the wavenumber spectrum is distorted, the frequency spectrum is unchanged.

e. Summary

Section 2a indicates that the frequency spectra of the distorted and undistorted scalar signals are equal in the limit of a steady velocity field:

$$\tilde{S}(f) = S(f). \tag{41}$$

In section 2b we relaxed the steady flow requirement and assumed that the time changes were due to the passage of turbulent eddies. Using turbulence scaling arguments, we then showed that the scalar frequency spectra are identical below the probe frequency $f_r = U_1/(2\pi a)$ if $(qa^{1/3})/(U_1 l^{1/3}) \ll 1$, which seems easily satisfied in typical aircraft applications. Meeting this criterion in tower measurements is more difficult.

In section 2c we restricted ourselves to high frequencies, where we argued that if $(qa)/(U_1\lambda) \ll 1$, which is probably typically satisfied only in the aircraft case, the turbulent flow near the probe should behave qualitatively as in rapid distortion. Our extension of the classical rapid-distortion analysis to a conservative scalar then showed that the frequency spectrum is again unchanged:

$$\tilde{S}(f) = S(f), \quad f \sim U_1/a. \tag{42}$$

In summary, we argue that for frequencies of order U_1/a and lower (which typically covers the band from the upper end of the inertial subrange to zero), and for typical conditions, the frequency spectrum of a conservative scalar measured ahead of aircraft is changed negligibly by probe-induced flow distortion. The situation for tower measurements is less clear, but it seems that under the most favorable conditions the spectrum will be essentially unchanged in that case as well.

3. Aircraft applications

a. Scalar density measurements

Some instruments, such as the Lyman-α hygrometer for water vapor and infrared radiation sensors for CO_2, measure scalar mass density ρ_s rather than scalar mixing ratio ρ_s/ρ. As we discussed earlier, mass density is not a strictly conservative quantity at aircraft speeds. We now investigate the effects of flow distortion on its time series.

We assume that the constraints summarized in 2e are satisfied, so that the time series of scalar mixing ratio measured near the radome is simply a time-lagged version of that in the free stream:

$$\frac{\tilde{\rho}_s}{\tilde{\rho}}(\mathbf{x}_m, t + \Delta t) = \frac{\rho_s}{\rho}(\mathbf{x}_0, t). \tag{43}$$

We now represent density as the sum of a mean part and a fluctuation, e.g., $\rho = \bar{\rho} + \rho'$. Since density fluctuations are quite small compared to mean values, when we substitute this decomposition into (43) and average we can neglect the moments of the fluctuations; this gives the mean relation $\bar{\tilde{\rho}}_s/\bar{\tilde{\rho}} = \bar{\rho}_s/\bar{\rho}$. Subtracting this mean relation from the total equation (or, equivalently, linearizing (43) about the mean) then gives the fluctuating equation

$$\tilde{\rho}_s' = \frac{\bar{\tilde{\rho}}}{\bar{\tilde{\rho}}}\rho_s' + \frac{\bar{\rho}_s}{\bar{\rho}}\left(\tilde{\rho}' - \frac{\bar{\tilde{\rho}}}{\bar{\rho}}\rho'\right), \tag{44}$$

where we have suppressed the arguments. Equation (44) shows that measured scalar density fluctuations are subject to two errors caused by the flow distortion. First, they are amplified by the ratio $\bar{\tilde{\rho}}/\bar{\rho}$, which at a stagnation point and an aircraft speed of 100 m s^{-1} is about 1.04. This can be easily corrected for, if necessary. Second, they are contaminated by "crosstalk" from fluctuations in air density; in fact, (44) shows that scalar density fluctuations will be induced in the flow-distortion region even if there are none in the free stream. Let us now assess this second effect.

We assume that the flow-distortion process is isentropic, so that density and temperature T before and after distortion are related by

$$\frac{\tilde{T}}{T} = \left(\frac{\tilde{\rho}}{\rho}\right)^{k-1}, \tag{45}$$

where k is the ratio of specific heats C_p/C_v. If we take differentials, representing temperature and density deviations about their means by T' and ρ', respectively, we find that

$$\tilde{\rho}' - \frac{\bar{\tilde{\rho}}}{\bar{\rho}}\rho' = \left(\frac{\bar{\rho}}{\bar{T}}\right)\frac{1}{(k-1)}\left(\frac{\bar{\tilde{\rho}}}{\bar{\rho}}\right)^{2-k}\left[\tilde{T}' - \left(\frac{\bar{\tilde{\rho}}}{\bar{\rho}}\right)^{k-1}T'\right]. \tag{46}$$

We now extend the quasi-steady, large-eddy flow distortion theory of Wyngaard (1981) to temperature, writing

$$\tilde{T}' = \left(\frac{\partial\tilde{T}}{\partial T}\right)_{U_i} T' + \left(\frac{\partial\tilde{T}}{\partial U_i}\right)_T u_i. \tag{47}$$

We can evaluate these derivatives by using the energy conservation equation

$$C_pT + \frac{U_jU_j}{2} = C_p\tilde{T} + \frac{\tilde{U}_j\tilde{U}_j}{2}. \tag{48}$$

Differentiating (48) with respect to T gives

$$\left(\frac{\partial\tilde{T}}{\partial T}\right)_{U_i} = 1 - \frac{\tilde{U}_j}{C_p}\frac{\partial\tilde{U}_j}{\partial T} = 1 + \frac{\tilde{U}_jM}{2C_pT}\frac{\partial\tilde{U}_j}{\partial M}, \tag{49}$$

where M is the free-stream Mach number $U_1/(kRT)^{1/2}$ with R the gas constant. The second term on the right-hand side of (49) represents the effects of compressibility; if we use the results of Van Dyke (1964), we find this term is of order $M^2U_1^2/(C_pT)$. Since typically $M \leqslant 0.3$ and $U_1^2/(C_pT) \leqslant 0.05$, it can be neglected. Differentiating (48) with respect to U_i gives

$$\left(\frac{\partial\tilde{T}}{\partial U_i}\right)_T = \frac{U_i}{C_p} - a_{ji}\frac{\tilde{U}_j}{C_p}. \tag{50}$$

Here a_{ij} is the flow-distortion tensor

$$a_{ij} = \left(\frac{\partial\tilde{U}_i}{\partial U_j}\right)_0, \tag{51}$$

(Wyngaard 1981), where the subscript 0 means evaluated at a steady, nonturbulent, equilibrium state. Combining (47), (49), and (50) gives

$$\tilde{T}' = T' + \frac{u_i}{C_p}(U_i - a_{ji}\tilde{U}_j). \tag{52}$$

Equation (52) states that the temperature fluctuation in the flow distortion region is the sum of the free-stream fluctuation (we assume that the eddy size is much larger than the radome, so the time-lag correction is unimportant), plus a linearized correction for kinetic energy changes between the free stream and the region of flow distortion. Equation (52) states that even if there are no temperature fluctuations in the free stream, temperature fluctuations will be induced in the distortion region by free stream velocity fluctuations. In the absence of flow distortion $\tilde{U}_j = U_j$ and $a_{ji} = \delta_{ji}$, the Kronecker delta, and (52) reduces to $\tilde{T}' = T'$.

If we now combine (44), (46), (48), and (52), and use the fact that density and temperature changes during flow distortion are small, we have

$$\tilde{\rho}_s' = \frac{\bar{\tilde{\rho}}}{\bar{\rho}}\rho_s' + \frac{\bar{\rho}_sU_1^2}{C_pT(k-1)} \times\left[-\frac{(1-\tilde{U}^2/U_1^2)T'}{2T} + \frac{(\delta_{1i} - a_{ji}\tilde{U}_j/U_1)u_i}{U_1}\right], \tag{53}$$

where we take the free stream velocity to be $U_i = U_1\delta_{1i}$ and $\tilde{U} = (\tilde{U}_i\tilde{U}_i)^{1/2}$ is the speed in the distortion region. Equation (53) indicates that the temperature crosstalk increases with the second power of mean air speed (i.e., flight speed) U_1, while the velocity crosstalk increases only linearly.

The contributions to the bracketed term in (53) are of order T'/T and q/U_1; these are typically no larger than 0.01. For $U_1 = 100$ m s^{-1}, the coefficient $U_1^2/(C_pT(k-1))$ is of order 0.1. Thus, the crosstalk term in (53) is of the order of $0.001\bar{\rho}_s$. While this seems small, if we are dealing with a scalar for which $\bar{\rho}_s \gg \rho_s'$ this crosstalk could be important.

Let us examine the effect of this crosstalk on the scalar density flux. We convert (53) to a flux equation by multiplying by u_3 and averaging; this gives

$$\overline{\tilde{\rho}_s'u_3} = \frac{\bar{\tilde{\rho}}}{\bar{\rho}}\overline{\rho_s'u_3} + \frac{\bar{\rho}_sU_1^2}{C_pT(k-1)} \times\left[-\frac{(1-\tilde{U}^2/U_1^2)\overline{T'u_3}}{2T} + \frac{(\delta_{1i} - a_{ji}\tilde{U}_j/U_1)\overline{u_iu_3}}{U_1}\right]. \tag{54}$$

This indicates that the measured scalar density flux

will be modified by the air density change during flow distortion and contaminated by crosstalk from the temperature flux $\overline{T'u_3}$ and the Reynolds stress $\overline{u_i u_3}$.

Let us now do a sample calculation for CO_2, a species whose density, rather than mixing ratio, is measured by most available sensors and whose flux is of interest. We take $\bar{\rho}_s = 0.6 \times 10^{-3}$ kg m^{-3} (Broecker et al. 1986), and we assume $U_1 = 100$ m s^{-1}. We consider first the temperature-induced crosstalk when the CO_2 sensor is located where $\tilde{U} \ll U_1$, and assume a measurement over the sea. In the convective marine boundary layer, the near-surface temperature flux ranges from 0.01 to 0.1 K m s^{-1} (Brost et al. 1982; Lenschow et al. 1980); we will use 0.03 K m s^{-1}. Equation (54) then indicates that the CO_2 flux error due to temperature crosstalk is about 1.2 mol m^{-2} yr^{-1}. Estimates of the zonal average net CO_2 flux vary from -3 (into the sea) to $+3$ (out of the sea) mol m^{-2} yr^{-1}, and local fluxes are not expected to be very much larger except under very special circumstances (Broecker et al. 1986). In this case, therefore, the magnitude of flux error induced by the temperature crosstalk is about 40%. This might be a worst case for the temperature-crosstalk effect. Although the temperature flux over land can be as much as a factor of 10 larger than the value we just used, the CO_2 flux is typically at least that much larger as well, making the relative error smaller than in our sample calculation.

Consider next the velocity crosstalk in (54). We write this as

$$\text{velocity error flux} = \frac{\bar{\rho}_s U_1^2}{C_p T(k-1)}\left[\left(1 - \frac{a_{j1}\tilde{U}_j}{U_1}\right)\frac{\overline{u_1 u_3}}{U_1} - \frac{a_{j2}\tilde{U}_j}{U_1}\frac{\overline{u_2 u_3}}{U_1} - \frac{a_{j3}\tilde{U}_j}{U_1}\frac{\overline{u_3 u_3}}{U_1}\right]$$

$$= \frac{\bar{\rho}_s U_1^2}{C_p T(k-1)}\left[F_1\frac{\overline{u_1 u_3}}{U_1} + F_2\frac{\overline{u_2 u_3}}{U_1} + F_3\frac{\overline{u_3 u_3}}{U_1}\right], \quad (55)$$

where

$$F_1 = 1 - \frac{a_{11}\tilde{U}_1}{U_1} - \frac{a_{21}\tilde{U}_2}{U_1} - \frac{a_{31}\tilde{U}_3}{U_1}, \quad (56)$$

$$F_2 = -\frac{a_{12}\tilde{U}_1}{U_1} - \frac{a_{22}\tilde{U}_2}{U_1} - \frac{a_{32}\tilde{U}_3}{U_1}, \quad (57)$$

$$F_3 = -\frac{a_{13}\tilde{U}_1}{U_1} - \frac{a_{23}\tilde{U}_2}{U_1} - \frac{a_{33}\tilde{U}_3}{U_1}. \quad (58)$$

Equation (55) shows that the velocity crosstalk effects depend on the details of the distortion geometry and the incoming turbulence field. To make these effects somewhat clearer, in Figs. 4 and 5 we show the behavior of F_1 and F_2 on concentric shells of 1.0, 1.1, and 2.0 radii upstream of a sphere. The plot of F_3 is that of F_2 rotated clockwise by 90 deg. These results are based on the a_{ij} calculated by Wyngaard (1981). Figures 4 and 5 show that although symmetry forces each of the F_i to vanish at some positions, there is no location where all three vanish.

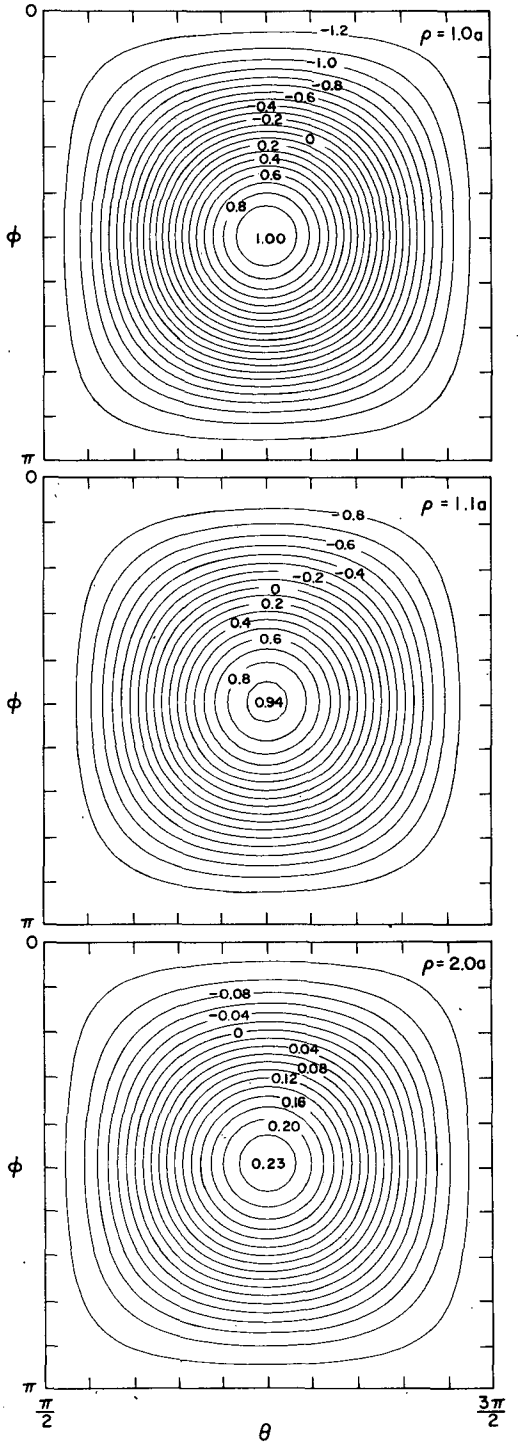

FIG. 4. Behavior of the distortion function F_1 defined in Eq. (55) on the $\rho = 1.0a$, $1.1a$, and $2.0a$ surfaces ahead of a sphere. The coordinates are defined in Fig. 3.

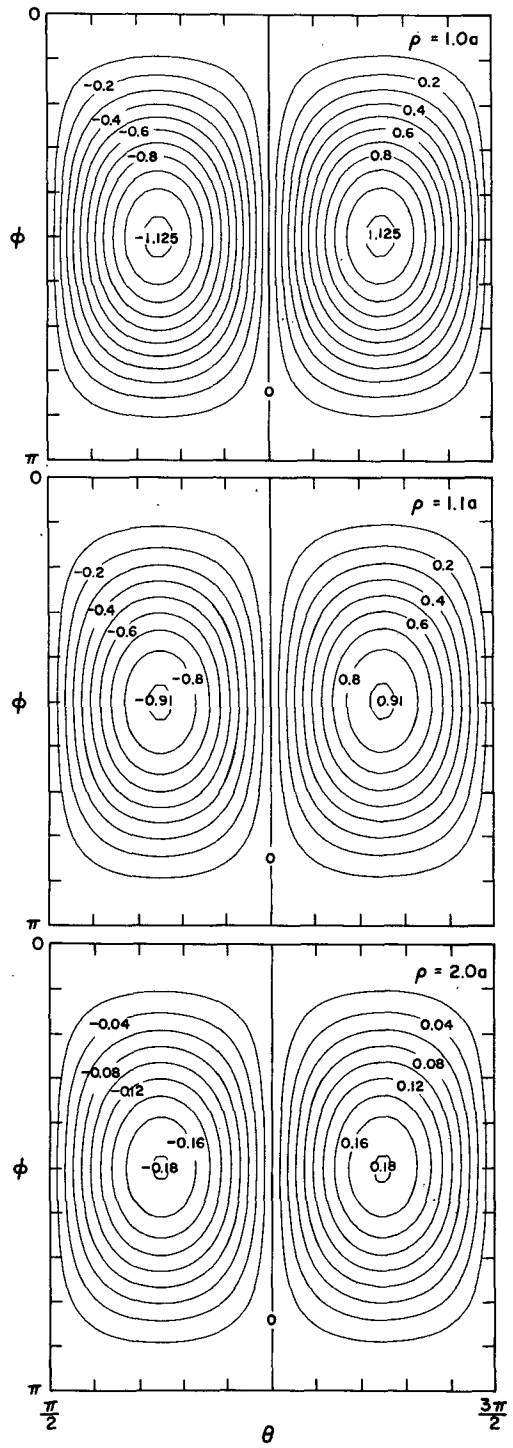

FIG. 5. Behavior of the distortion function F_2 defined in Eq. (55) on the $\rho = 1.0a$, $1.1a$, and $2.0a$ surfaces ahead of a sphere. F_3 plot is rotated clockwise 90 degrees.

Let us quickly estimate the magnitude of the velocity error flux indicated by (55). In applications to aircraft fitted with a nose radome rather than a boom the sensor would presumably be located off the centerline, in order to avoid disturbing the radome pressure ports. A "worst case" for crosstalk would result from locating it on the vertical center plane and near the radome skin, where Fig. 5 indicates that the magnitude of F_3 is maximum. From (55) this introduces contamination from both $\overline{u_1 u_3}$ and $\overline{u_3 u_3}$, but assume we measure in convective conditions when the latter is much the larger. We then have from (55)

$$\text{velocity error flux} \sim \frac{\bar{\rho}_s \tilde{U}_1 F_3 \overline{u_3 u_3}}{C_p T(k-1)}. \qquad (59)$$

For $\overline{u_3 u_3} = 1\ \text{m}^2\ \text{s}^{-2}$, $\tilde{U}_1 = 100\ \text{m s}^{-1}$, and $F_3 = 1.0$, (59) shows that the velocity-induced error in measured CO_2 flux is about 300 mol $\text{m}^{-2}\ \text{yr}^{-1}$. By comparison, Broeker et al. (1986) report that CO_2 fluxes during daylight hours over vegetated land surfaces range from 100 to 1000 mol $\text{m}^{-2}\ \text{yr}^{-1}$. Thus, the velocity-induced error in CO_2 flux can be as large as the flux itself. In near-neutral or slightly stable conditions $\overline{u_3 u_3}$ is typically an order of magnitude smaller, so that the error flux is perhaps 30 mol $\text{m}^{-2}\ \text{yr}^{-1}$. In each case this is larger than our estimate of the temperature-induced error. We conclude that the velocity-induced error is probably the more important of the two, and could pose serious limitations on the reliable measurement of CO_2 fluxes from aircraft.

Let us now consider the situation for water vapor flux measurements. If the sensor detects water vapor density, rather than mixing ratio, then (59) is a worst-case estimate of the flux error due to velocity crosstalk. For the conditions just used for CO_2, and for a mean water vapor density of 10 g m^{-3}, the error flux is 0.01 g $\text{m}^{-2}\ \text{s}^{-1}$ (about 0.3 m yr^{-1}). This is 30% of the global-average water vapor flux of 1.0 m yr^{-1} (Brutsaert 1982). Local water vapor fluxes can vary over a wide range, of course; values as large as 0.30 g $\text{m}^{-2}\ \text{s}^{-1}$ (10 m yr^{-1}) were measured in the convective boundary layer formed by cold air outbreaks over the warm sea in AMTEX (Lenschow et al. 1980), and values a few percent of that can occur over arid land. Thus, the velocity component of the crosstalk flux could cause significant errors in water-vapor fluxes measured from aircraft. Later we will discuss possible strategies for dealing with these errors.

b. *Temperature measurements*

We assume that within the flow distortion region the measured temperature T^m and the true temperature $\tilde{T}$ are related by the thermometer recovery factor r, defined as

$$r = 2C_p \frac{T^m - \tilde{T}}{\tilde{U}^2}. \qquad (60)$$

Equation (48) for energy conservation and (60) give our basic relation

$$T^m = T + \frac{U_1^2}{2C_p} - \frac{\tilde{U}^2}{2C_p}(1 - r). \tag{61}$$

If the thermometer is "perfect", i.e., has $r = 1$, (61) shows that it measures the correct stagnation temperature, $T + U_1^2/(2C_p)$. If not, its error depends not only on $(1 - r)$, but also on the distorted mean speed at the measurement point. Both these factors can vary with the approach flow, which fluctuates slightly due to the turbulence in the free stream. This indicates that free-stream velocity fluctuations generate measured temperature fluctuations if $r \neq 1$. We will now investigate this mechanism.

We write (61) as

$$\Delta = T^m - T = \frac{U_1^2}{2C_p} - \frac{\tilde{U}^2}{2C_p}(1 - r) = \Delta(\tilde{U}, r, U_1). \tag{62}$$

Let there be a velocity fluctuation $u_i = (u_1, u_2, u_3)$ in the free stream, and let its spatial scale be very large compared to the radome scale a so that the distorted flow has time to adjust to the new speed and direction. Now $u_i \ll U_1$, and we assume the resulting fluctuations in $\tilde{U}_i$, r, and U_1 are also small. Thus, we can approximate the fluctuating temperature difference signal as the differential of Δ:

$$T'^m - T' \approx d\Delta = \frac{\partial \Delta}{\partial \tilde{U}} d\tilde{U} + \frac{\partial \Delta}{\partial r} dr + \frac{\partial \Delta}{\partial U_1} dU_1$$

$$= d\Delta_1(\tilde{U}) + d\Delta_2(r) + d\Delta_3(U_1). \tag{63}$$

Let us now examine the three contributions to $T'^m - T'$.

Starting from the definition of the first contribution,

$$d\Delta_1 = \frac{\partial \Delta}{\partial \tilde{U}} d\tilde{U}, \tag{64}$$

we write from (62)

$$d\Delta_1 = \frac{\partial \Delta}{\partial \tilde{U}} \frac{\partial \tilde{U}}{\partial U_i} u_i = (r - 1) \frac{\tilde{U}}{C_p} \frac{\partial \tilde{U}}{\partial U_i} u_i. \tag{65}$$

From the relation $\tilde{U}^2 = \tilde{U}_1^2 + \tilde{U}_2^2 + \tilde{U}_3^2$ we have

$$\frac{\partial \tilde{U}}{\partial U_i} = \frac{\tilde{U}_j}{\tilde{U}} a_{ji}, \tag{66}$$

where a_{ij} is the flow-distortion matrix defined in (51) and introduced by Wyngaard (1981). From (65) and (66) we then have

$$d\Delta_1 = (r - 1) \frac{\tilde{U}_j}{C_p} a_{ji} u_i. \tag{67}$$

For the second contribution, we assume $r = r(\alpha_1, \alpha_2)$ where α_1 and α_2 are the angles that define the flow vector with respect to the thermometer. Thus, we write

$$d\Delta_2 = \frac{\partial \Delta}{\partial r} dr = \frac{\tilde{U}^2}{2C_p} \frac{\partial r}{\partial \alpha_j} \frac{\partial \alpha_j}{\partial U_i} u_i. \tag{68}$$

For the third contribution we have directly from (62)

$$d\Delta_3 = \frac{\partial \Delta}{\partial U_1} dU_1 = \frac{U_1}{C_p} u_1 = \frac{U_1}{C_p} u_i \delta_{1i}. \tag{69}$$

Combining (63) with (67)–(69) and rearranging then gives

$$T'^m - T' = \frac{U_1}{C_p}\left[(1 - r)(\delta_{1i} - a_{ji}\tilde{U}_j/U_1) + r\delta_{1i} + \frac{\tilde{U}^2}{2U_1} \frac{\partial r}{\partial \alpha_j} \frac{\partial \alpha_j}{\partial U_i}\right] u_i. \tag{70}$$

The first term on the right-hand side of (70) represents the temperature error caused by free-stream velocity changes in the presence of flow distortion and a recovery factor less than 1.0. The second term represents purely the effect of free-stream velocity fluctuations; since it is not related to flow distortion we will not consider it an error term but assume instead that it is removed in data processing. The final term represents the effect of recovery factor changes as the flow direction at the sensor changes in response to direction changes in the free stream.

Let us examine the implications of the flow-distortion errors indicated by (70) for temperature flux measurements. Multiplying (70) by vertical velocity u_3 and averaging gives

$$\overline{T'u_3}^m = \overline{T'u_3} + \frac{U_1}{C_p}\left[(1 - r)(F_1\overline{u_1u_3} + F_2\overline{u_2u_3} + F_3\overline{u_3u_3}) + \frac{\tilde{U}^2}{2U_1} \frac{\partial r}{\partial \alpha_j} \frac{\partial \alpha_j}{\partial U_i} \overline{u_iu_3}\right]. \tag{71}$$

The second term on the right of (71) is the error due to the direction sensitivity of the temperature probe. It appears that very little is known about this, but if the probe is operated within its design range this term is presumably negligible. Thus, the velocity-induced crosstalk errors for scalar density flux, Eq. (55), and temperature flux, Eq. (71), have the same dependence on flow-distortion parameters, so sensors for these fluxes share the same set of optimum design criteria.

c. *Design criteria for scalar flux measurements*

The form of the velocity-induced flux errors (55) and (71) and the behavior of their flow-distortion parameters F_1, F_2 and F_3 (Figs. 4 and 5) suggest the

advantages of the traditional center-mounted, forward-pointing nose boom. If the scalar measurements are made on the centerline ahead of an axisymmetric body, F_2 and F_3 vanish by symmetry. On the axis ahead of a sphere, F_1 behaves as (Wyngaard 1981)

$$F_1 = 1 - a_{11}^2 = 1 - (1 - |x_1/a|^{-3})^2. \quad (72)$$

Thus, F_1 can be made as small as desired by extending the measurement point upward from the body. Equation (72) indicates that F_1 is 1.0, 0.94, and 0.23 at 1.0, 1.1, and 2.0 radii upstream, as shown in Fig. 4; it decreases to 0.07 and 0.03 at 3.0 and 4.0 radii upstream, respectively.

An alternative is to mount the scalar species sensor closer to the aircraft but in a vertically symmetric geometry so that $F_3 = 0$. This could be achieved by mounting it on one side of the horizontal midplane of the nose radome, for example. In this case (55) and (71) indicate velocity crosstalk errors proportional to $F_1\overline{u_1u_3} + F_2\overline{u_2u_3}$. While potentially important, these change sign as the flight path direction is reversed. Averaging scalar density fluxes from flights in opposite directions will in principle remove these errors. In practice, however, they will not completely cancel for two reasons. First, boundary-layer flow is almost never stationary; Reynolds stress changes with time, and, hence, will differ in runs separated in time. Second, the ensemble average stress changes sign, but the leg-average value is only an approximation to that; thus, values from opposing legs will not average precisely to zero in each realization. As a result, the F_1 and F_2 terms will add essentially zero-mean noise (i.e., scatter) to the measured scalar fluxes.

Another alternative, due to W. A. Cooper and J. Weil (personal communication), is to use two scalar species sensors on the horizontal midplane (where $F_3 = 0$) mounted symmetrically about the centerline (where F_2 values are of opposite sign). Averaging the two scalar species time signals would then remove the F_2 error.

Equation (54) shows that scalar density fluxes also suffer from an error due to temperature crosstalk. The flow-distortion part of this error is proportional to $(1 - \tilde{U}^2/U_1^2)$. Along the centerline ahead of a sphere this reduces to (72), which, as we saw, is negligible sufficiently far upstream. Nearer the body it is positive, reaching 1.0 at the stagnation point; it decreases downstream from that, passes through 0 at $x_1/a = -\sqrt{3}/3$, and becomes negative farther downstream where $\tilde{U} > U_1$. Thus, this term can also be minimized through design.

4. Summary and conclusions

In this paper we addressed the question: What is the relation between the time series of a scalar in a region of probe-induced flow distortion and that in the free stream? For conservative scalars measured under typical conditions on towers and from research aircraft, we found that the answer can be surprisingly simple. If conditions are sufficiently steady, the dot product of scalar gradient and fluid velocity is conserved during flow distortion; this implies that the time series is unaffected except for a time lag. We found that typical aircraft applications meet the "sufficiently steady" criteria. They are more difficult, but not impossible, to meet in tower applications. It is important that these conclusions be tested experimentally.

The high speeds in aircraft applications when coupled with flow distortion can cause serious errors in measured fluxes of nonconservative scalars such as the density of water vapor and trace species. The error path is as follows. Total mixing ratio is conserved in flow distortion, so that species density fluctuations at the measurement point are due both to mixing ratio fluctuations (which are essentially unchanged from the free stream value) and air density fluctuations. Air density fluctuations, in turn, depend on temperature and velocity fluctuations and on the distortion of the velocity field. Thus, the measured species density signal is contaminated by both temperature and velocity, the magnitude of the contamination depending on the velocity distortion. As a result, the measured species density flux is contaminated by both the temperature flux and the Reynolds stress. The physics of the error in measured temperature flux is similar but depends also on the deviation of the thermometer recovery factor from 1.0.

These flux errors can be important for CO_2 and water vapor, but they can be minimized by avoiding flow distortion. One approach is the traditional one of mounting the sensors on sufficiently long booms upwind of the aircraft. It might also be possible to minimize scalar flux errors while mounting sensors closer to the aircraft if close attention is paid to the details of the flow-distortion effects.

Acknowledgments. I am grateful to W. A. Cooper and D. H. Lenschow for numerous discussions about aircraft measurements; to E. Novikov for discussions about rapid distortion; to J. Businger, M. A. LeMone, R. Rotunno, and J. Weil for comments on a draft manuscript; and to P. Pinkney for generating the computer plots of the F_i.

REFERENCES

Batchelor, G. K., and I. Proudman, 1954: The effect of rapid distortion of a fluid in turbulent motion. *Quart. J. Mech. Appl. Math.*, 7, Part 1, 83–103.

Broecker, W., J. R. Ledwell, T. Takahashi, R. Weiss, L. Merlivat, L. Memery, T. H. Peng, B. Jahne and K. O. Munnich, 1986: Isotopic versus micrometeorologic ocean CO_2 fluxes: A serious conflict. *J. Geophys. Res.*, **91**(C9), 10517–10527.

Brost, R. A., D. H. Lenschow and J. C. Wyngaard, 1982: Marine stratocumulus layers. Part I: Mean conditions. *J. Atmos. Sci.*, **39,** 800–817.

Brown, E. N., C. A. Friehe and D. H. Lenschow, 1983: The use of pressure fluctuations on the nose of an aircraft for measuring air motion. *J. Climate Appl. Meteor.*, **22,** 171–180.

Brutsaert, W., 1982: *Evaporation into the Atmosphere.* D. Reidel, 299 pp.

Champagne, F. H., C. A. Friehe, J. C. LaRue and J. C. Wyngaard, 1977: Flux measurements, flux estimation techniques, and fine-scale turbulence measurements in the unstable surface layer over land. *J. Atmos. Sci.*, **34,** 515–530.

Hogstrom, U., 1982: A critical evaluation of the aerodynamic error of a turbulence instrument. *J. Appl. Meteor.*, **21,** 1838–1844.

Hunt, J. C. R., 1973: A theory of turbulent flow round two-dimensional bluff bodies. *J. Fluid Mech.*, **61,** 625–706.

Lenschow, D. H., J. C. Wyngaard and W. T. Pennell, 1980: Mean-field and second-moment budgets in a baroclinic, convective boundary layer. *J. Atmos. Sci.*, **37,** 1313–1326.

Lumley, J. L., 1965: The interpretation of time spectra measured in high-intensity shear flows. *Phys. Fluids,* **8,** 1056–1062.

——, and H. A. Panofsky, 1964: *The Structure of Atmospheric Turbulence.* Wiley Interscience, 300 pp.

Tennekes, H., and J. L. Lumley, 1972: *A First Course in Turbulence.* MIT Press, 300 pp.

Van Dyke, M., 1964: *Perturbation Methods in Fluid Mechanics.* Academic Press, 229 pp.

Wyngaard, J. C., 1981: The effects of probe-induced flow distortion on atmospheric turbulence measurements. *J. Appl. Meteor.*, **20,** 784–794.

——, 1986: Measurement physics. *Probing the Atmospheric Boundary Layer,* D. H. Lenschow, Ed., Amer. Meteor. Soc., 269 pp.

——, 1988: Flow-distortion effects on scalar flux measurements in the surface layer: Implications for sensor design. *Bound.-Layer Meteorol.*, **42,** 19–26.

——, L. Rockwell and C. A. Friehe, 1985: Errors in the measurement of turbulence upstream of an axisymmetric body. *J. Atmos. Oceanic Technol.*, **2,** 605–614.